d-Wave Pairing in the Presence of Long-Range Coulomb Interactions

Gökhan Esirgen,[1,*] H.-B. Schüttler,[1] and N. E. Bickers[2]

[1]*Center for Simulational Physics, Department of Physics and Astronomy, University of Georgia, Athens, Georgia 30602-2451*
[2]*Department of Physics and Astronomy, University of Southern California, Los Angeles, California 90089-0484*

The one-band extended Hubbard model in two dimensions near band-filling $\frac{1}{2}$ is solved in the fluctuation exchange approximation, including the long-range $(1/r)$ part of the Coulomb interaction, up to 4th-neighbor distance. Our results suggest that $d_{x^2-y^2}$ pairing in the Hubbard model is robust against the inclusion of long-range Coulomb interactions with moderate 1st-neighbor repulsion strength V_1. $d_{x^2-y^2}$ pairing is suppressed only at large V_1 ($\gtrsim 0.25U - 0.4U$), due to incipient charge density wave instabilities. [S0031-9007(99)08467-7]

Several cuprate superconductors appear to exhibit a pairing state of $d_{x^2-y^2}$ symmetry [1]. Such a non-*s*-wave state was also found early on in microscopic pairing theories, based on antiferromagnetic (AF) spin correlations in the two-dimensional (2D) Hubbard model [2]. While incorporating the local on-site U Coulomb repulsion, the Hubbard-based $d_{x^2-y^2}$ pairing theories have so far largely ignored the effects of the spatially more extended Coulomb matrix elements. Although unaffected by the on-site U, non-*s*-wave pairing states can, in principle, be severely suppressed by the longer-range Coulomb repulsion, due to the spatially extended nature of their Cooper pair wave functions. For any pairing theory it is therefore of central importance to establish whether non-*s*-wave pairing survives the extended repulsion.

Here, we address this question in a self-consistent diagrammatic framework, the fluctuation exchange (FLEX) approximation [3], applied to an *extended* Hubbard model. We show that $d_{x^2-y^2}$ pairing is (i) robust against extended Coulomb terms of realistic strength and (ii) suppressed only if the extended repulsion becomes so strong that it induces charge density wave (CDW), rather than AF spin density wave (SDW), instabilities in the $\frac{1}{2}$-filled Hubbard system. This CDW scenario is apparently not realized in the undoped cuprates [2].

We start from the 2D extended Hubbard Hamiltonian,

$$\mathcal{H} = \sum_{ij}\left(-\sum_{\sigma} t_{ij}c_{i\sigma}^{\dagger}c_{j\sigma} + \frac{1}{2}\sum_{\sigma\sigma'} V_{ij}n_{i\sigma}n_{j\sigma'}\right), \quad (1)$$

where $c_{i\sigma}^{\dagger}$ creates a hole with spin σ at site $\mathbf{R}_i$ on an $N = L \times L$ square lattice with periodic boundary conditions, and $n_{i\sigma} = c_{i\sigma}^{\dagger}c_{i\sigma}$. In t_{ij}, we include only a 1st-neighbor hybridization t and the chemical potential μ. The Coulomb matrix element $V_{ij} \equiv V(\mathbf{R}_i - \mathbf{R}_j)$ com-

prises the Hubbard on-site repulsion $U \equiv V(\mathbf{0})$ and an extended $1/r$ part, $V(\Delta\mathbf{R}) = V_1/|\Delta\mathbf{R}|$ for $0 < |\Delta\mathbf{R}| \leq r_n$, up to the nth-neighbor distance r_n. Here V_1 denotes the strength of the 1st-neighbor repulsion and $\Delta\mathbf{R}$ is in units of the lattice constant a with $a \equiv 1$ in the following. For the cuprates, we assume $t \sim 0.3 - 0.5$ eV and $U/t \sim 8 - 12$ [4,5]. Absorbing dielectric screening effects from the insulating non-Hubbard electron background into an effective V_1, one estimates $V_1/t \lesssim 2 - 3$ [6]. Additional screening from phonons reduces this to $V_1/t \lesssim 0.3 - 0.5$ [6] but should really be treated explicitly in a more realistic electron-phonon model, because of the low (i.e., potentially relevant) phonon energy scale.

In Fig. 1(a), we show typical (3rd order) FLEX contributions to the single-particle self-energy Σ, written in terms of the bare particle-hole vertices V_d for density and V_m for magnetic fluctuation exchange. In Figs. 1(b) and 1(c), we show the bare vertex V_s and, respectively, the 1st and typical higher (3rd) order contributions to the renormalized vertex Γ_s for the singlet particle-particle interaction. We do not include particle-particle fluctuation exchange in Σ. Hence, within our FLEX approximation [3], no Aslamazov-Larkin-type diagrams [3,7] contribute to Γ_s at or above T_c (see also previous applications in Ref. [8]).

The finite cutoff, $V(\Delta\mathbf{R}) \equiv 0$ for $|\Delta\mathbf{R}| > r_n$, makes a numerical solution of the FLEX equations [3] feasible. The key algorithmic ingredients are (i) introduction of a mixed real-space and momentum-space basis set [9,10] for two-body propagators and (ii) application of a numerical renormalization group to calculate Matsubara frequency sums [8]. The vertices (V_d, V_m, V_s) are $M \times M$ matrices, where M is the number of $\Delta\mathbf{R}$ with $V(\Delta\mathbf{R}) \neq 0$. For example, in the 1st-neighbor ($n = 1$) Coulomb model, $M = 5$ and their nonzero matrix elements at $Q \equiv (\mathbf{Q}, \Omega)$ [see Figs. 1(a) and 1(b)] are

$$V_d(Q; \Delta\mathbf{R}; \Delta\mathbf{R}') = \begin{cases} U + 4V_1(\cos Q_x + \cos Q_y), & \Delta\mathbf{R} = \Delta\mathbf{R}' = \mathbf{0}, \\ -V_1, & \Delta\mathbf{R} = \Delta\mathbf{R}' = \pm\hat{x}, \pm\hat{y}, \end{cases} \quad (2)$$

$$V_m(Q; \Delta\mathbf{R}; \Delta\mathbf{R}') = \begin{cases} -U, & \Delta\mathbf{R} = \Delta\mathbf{R}' = \mathbf{0}, \\ -V_1, & \Delta\mathbf{R} = \Delta\mathbf{R}' = \pm\hat{x}, \pm\hat{y}, \end{cases} \quad (3)$$

$$V_s(Q; \Delta \mathbf{R}; \Delta \mathbf{R}') = \begin{cases} U, & \Delta \mathbf{R} = \Delta \mathbf{R}' = \mathbf{0}, \\ V_1/2, & \Delta \mathbf{R} = \pm \Delta \mathbf{R}' = \pm \hat{x}, \pm \hat{y}. \end{cases} \qquad (4)$$

The superconducting transition occurs when $\lambda^s = 1$, where λ^s is the largest eigenvalue of the integral kernel for the particle-particle ladder series with Γ_s as the interaction vertex [3] at total pair momentum-energy $Q_s = 0$. The T_c results reported here are for 16×16 lattices and agree with 32×32 lattice results to within 5% at selected parameter values we have checked.

In Fig. 2 we plot the superconducting transition temperature T_c as a function of V_1 for different hole concentrations and different U in the 1st-neighbor ($n = 1$) and 2nd-neighbor ($n = 2$) Coulomb repulsion models. As in previous FLEX calculations for Hubbard-like models, the symmetry of the dominant pairing instability is $d_{x^2-y^2}$ [2,8,9,11]. The striking feature in Fig. 2 is the remarkable insensitivity of T_c to V_1 over a wide parameter range. An eventual abrupt downturn in T_c occurs only when V_1 approaches the crossover V_1^{md} from SDW to CDW fluctuation behavior, discussed below.

To understand this behavior, we analyze the decomposition of Γ_s in Fig. 1(c) for the case of the 1st-neighbor

($n = 1$) model. We consider $\Gamma_s(0; \Delta \mathbf{R}, i\pi T; \Delta \mathbf{R}, i\pi T)$ as a measure of the effective interaction between holes separated by $\Delta \mathbf{R}$ in the $Q_s = 0$ singlet pairing channel at temperature T. Note that V_1 affects T_c via the 1st order (Hartree-Fock) contribution to Σ (not shown in Fig. 1), via the 1st order contribution V_s [Fig. 1(c)] to Γ_s, and via the charge and spin fluctuation contributions, that is, via the V_d- and V_m-ladder series which enter into Σ [Fig. 1(a)] and Γ_s [Fig. 1(c)].

The primary reason for the robustness of the d-wave pairing against moderate 1st-neighbor repulsions, $V_1 \lesssim V_1^{md}$, is simply the raw strength of the effective electron-electron interaction generated by the spin fluctuations, primarily with momentum transfer $\mathbf{Q}$ [see Fig. 1(a)] near $\mathbf{Q} = (\pi, \pi)$. For example, at 1st-neighbor distance, $U = 8t$ and hole density $\langle n \rangle \equiv \langle \sum_\sigma n_{j\sigma} \rangle = 1.16$; this attractive contribution to Γ_s is of order $32t$. This clearly dominates over extended Coulomb effects at moderate V_1.

At $U = 8t$, the primary effect of a moderate V_1 on Γ_s is a slight enhancement of the 1st-neighbor attraction, by
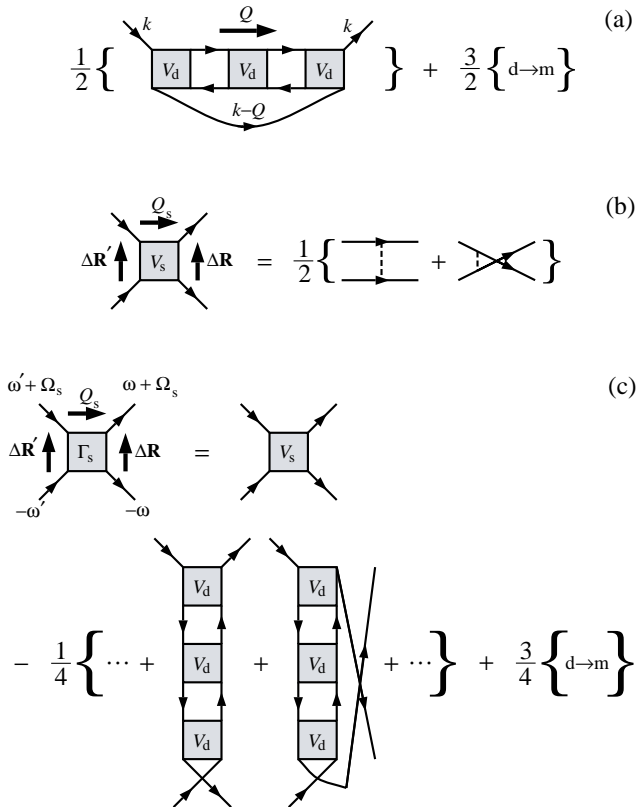

FIG. 1. Diagrams included in the FLEX approximation: (a) Representative higher (3rd) order contribution to the fluctuation self-energy $\Sigma(k)$. (b) Bare singlet pairing vertex, $V_s(Q_s; \Delta \mathbf{R}; \Delta \mathbf{R}')$, with total pair momentum-energy $Q_s \equiv (\mathbf{Q}_s, \Omega_s)$. (c) 1st and typical higher (3rd) order contributions to the full singlet pairing vertex, $\Gamma_s(Q_s; \Delta \mathbf{R}, \omega; \Delta \mathbf{R}', \omega')$.
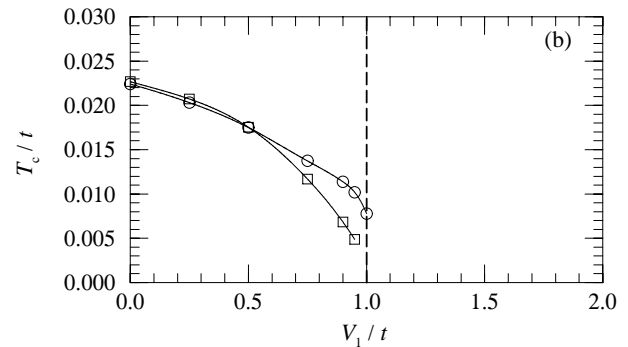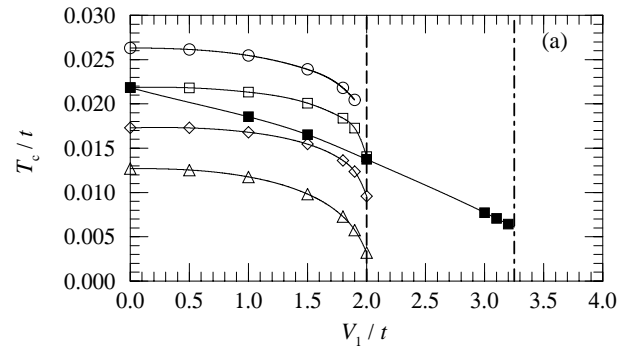

FIG. 2. $d_{x^2-y^2}$ transition temperature T_c vs 1st-neighbor Coulomb repulsion, V_1, at (a) $U = 8t$ and (b) $U = 4t$ for hole densities $\langle n \rangle = 1.12$ (circles), 1.16 (squares), 1.20 (diamonds), and 1.24 (triangles). Open symbols are for the 1st-neighbor ($n = 1$), closed symbols for the 2nd-neighbor ($n = 2$) Coulomb model. Vertical dashed (dot-dashed) lines mark the crossover V_1^{md} from SDW to CDW fluctuation behavior in the 1st-neighbor (2nd-neighbor) model, as described in text.

net amounts $\lesssim 0.2t$. This additional V_1-induced attraction is caused by $\mathbf{Q} \sim \mathbf{0}$ charge and by $\mathbf{Q} \sim (\pi, \pi)$ spin fluctuation contributions to Γ_s, which overscreen the direct 1st order repulsive Γ_s contribution, V_s, in Fig. 1(c). The reason for the slight suppression of T_c by a moderate V_1 at $U = 8t$ is therefore *not* the V_1 effect on Γ_s, but rather its effect on Σ. By increasing Σ, V_1 suppresses the single-particle spectral weight near the Fermi energy which, in turn, tends to reduce T_c. This Σ effect outweighs the Γ_s effect of V_1.

As indicated by the $U = 4t$ results in Fig. 2(b), a large U value is important for stabilizing the $d_{x^2-y^2}$ pairing against extended Coulomb effects. To understand this, note first that the spin fluctuation contributions to Γ_s and Σ are strongly U dependent. For example, at $U = 4t$, $V_1 = 0$ and $\langle n \rangle = 1.16$, the 1st-neighbor attraction induced by the spin fluctuations in Γ_s is reduced to $3.47t$, compared to $\sim 32t$ in the $U = 8t$ case. Despite this order of magnitude decrease, T_c for $U = 4t$ is slightly higher, due to the accompanying reduction of the self-energy effects discussed above. However, for this $U = 4t$ parameter set, T_c is also suppressed much more rapidly by turning on V_1. This is due to the fact that the spin fluctuation contribution to the 1st-neighbor attraction in Γ_s is now suppressed, rather than enhanced, by V_1. As a consequence, the net effect of V_1 on Γ_s is to suppress the 1st-neighbor attraction, for example, by about $0.6t$ for $V_1 = 0.5V_1^{\mathrm{md}}$. Because of the reduced overall strength of Γ_s, this is a relatively much larger effect than in the $U = 8t$ case and therefore has a much larger effect on T_c.

The SDW-CDW crossover V_1^{md} in Fig. 2 is operationally defined as that V_1 value where the maximal "density" eigenvalue λ^d becomes equal to the maximal "magnetic" eigenvalue λ^m. Here, λ^d and λ^m denote, respectively, the largest eigenvalues of the integral kernels for the V_d- and V_m-based particle-hole ladder series entering into Σ and Γ_s, shown in Figs. 1(a) and 1(c). This criterion for V_1^{md} may give only rough estimates of the actual physical crossover since, instead of the full interaction vertices Γ_d and Γ_m [3], it is obtained from the bare interaction vertices V_d and V_m. The estimates are reasonable *vis-à-vis* $t \to 0$ limit results discussed below.

As V_1 approaches V_1^{md}, CDW fluctuations rapidly take over and due to their nearly singular nature preclude convergence of our self-energy iteration for $T \lesssim 0.1t$ and $V_1 > V_1^{\mathrm{md}}$. In the 1st-neighbor ($n = 1$) Coulomb model, the CDW fluctuations exhibit maximum λ^d near $\mathbf{Q} = (\pi, \pi)$. They produce a repulsive 1st-neighbor contribution to Γ_s, *and*, via Σ, they weaken the strength of the attractive $\mathbf{Q} \sim (\pi, \pi)$ spin fluctuation contribution to Γ_s when $V_1 \to V_1^{\mathrm{md}}$. The $\mathbf{Q} \sim (\pi, \pi)$ charge fluctuations also generate an on-site attraction which is too weak, however, to overcome the on-site repulsion due to U and $\mathbf{Q} \sim (\pi, \pi)$ spin fluctuations. No pairing instabilities are found down to $T \sim 0.1t$ for $V_1 > V_1^{\mathrm{md}}$; the dominant attractive symmetries are odd-ω s wave in the triplet and

even-ω s wave in the singlet channel with respective pairing eigenvalues $\lambda^t \sim 0.35-0.45$ and $\lambda^s \sim 0.25-0.4$ in the $10\%-20\%$ doping range. $d_{x^2-y^2}$ pairing is suppressed. The singlet s-wave attraction suggests that CDW fluctuations may enhance conventional phonon-mediated pairing. In the 2nd-neighbor ($n = 2$) Coulomb model, the SDW-CDW crossover is similar, but driven by CDW fluctuations with maximum λ^d near $\mathbf{Q} = (0, \pi)$ and $(\pi, 0)$.

The physical origin of the SDW-CDW crossover can be understood by considering the exactly solvable ionic limit, $t \to 0$, at $\frac{1}{2}$ filling [5]. Large U favors a ground state with single occupancy at each site and AF SDW order for $|t| = 0^+$. Large V_1, in the 1st-neighbor Coulomb model, favors a CDW ground state with modulation wave vector $\mathbf{Q}^* = (\pi, \pi)$ and alternating double and zero occupancy in the respective two sublattices. The transition between these two states occurs when V_1 reaches [5] $V_1^{\mathrm{md}|t=0} = \frac{1}{4}U$ which coincides with the exact crossover $V_1^{\mathrm{md}} = \frac{1}{4}U$ shown in Fig. 2. In the 2nd-neighbor Coulomb model, the competing CDW state has $\mathbf{Q}^* = (0, \pi)$ or $(\pi, 0)$, with alternating doubly and zero occupied rows or columns, and the transition occurs at $V_1^{\mathrm{md}|t=0} = \sqrt{2}U/4 \cong 0.354U$. This is roughly consistent with the approximately T- and $\langle n \rangle$-independent crossover $V_1^{\mathrm{md}} \simeq 0.406U$ from Fig. 2(a). This analysis suggests that the crossover is driven by incipient CDW instabilities in the $\frac{1}{2}$-filled Mott-Hubbard insulator. We emphasize that such CDW instabilities and their effects on pairing *cannot* be treated in strong-coupling versions of the Hubbard model, such as the t-J model [12]. CDW fluctuations in the $\frac{1}{2}$-filled system are precluded from the outset by the no-double-occupancy Hilbert space constraints imposed in such models.

By exploiting the retarded nature of the pairing potential, the pair wave function can evade the destructive effects of the instantaneous Coulomb repulsion [13], provided the characteristic frequency Ω_B of the pairing-mediating boson is much lower than characteristic electronic energy scales such as the Fermi energy ϵ_F. This Coulomb "pseudopotential" effect [13] is crucial for conventional phonon-mediated superconductors, where $\Omega_B/\epsilon_F \sim 10^{-2}-10^{-3}$. However, in the present problem, $\Omega_B/\epsilon_F \sim 10^{-1}$ is *not* very small, since the spin fluctuation frequencies Ω_B extend up to a sizable fraction of the electronic bandwidth [8,14,15]. By a variational analysis, based on restricted trial pair wave functions, we can indeed show that the pseudopotential effect raises λ^s and T_c by no more than a few percent; i.e., it is largely inoperative in spin fluctuation mediated pairing.

Next, we consider longer-range $1/r$ Coulomb terms. As shown in Fig. 2(a), the inclusion of 2nd-neighbor ($n = 2$) Coulomb terms suppresses T_c more strongly at low V_1 than in the 1st-neighbor model. However, the d-wave pairing also survives to larger V_1, since V_1^{md} is increased in the 2nd-neighbor model. Comparable V_1^{md} are found in longer-range models with $n > 2$.
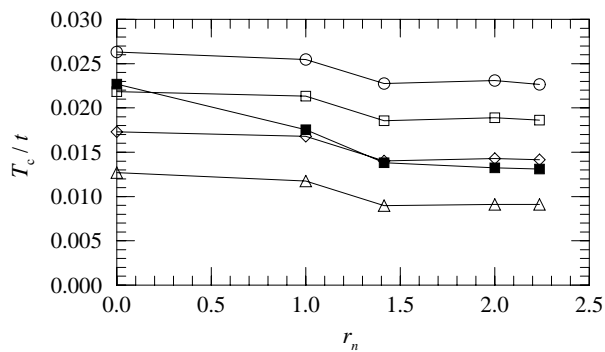
FIG. 3. $d_{x^2-y^2}$ T_c vs cutoff radius r_n of the extended Coulomb interaction. Here, $r_n = 0, 1, \sqrt{2}, 2$, and $\sqrt{5}$, for $n = 0, 1, 2, 3$, and 4th-neighbor cutoff, respectively. Open symbols are for $U/t = 8$, $V_1/t = 1$; closed symbols are for $U/t = 4$, $V_1/t = 0.5$, with $\langle n \rangle = 1.12$ (circles), 1.16 (squares), 1.20 (diamonds), and 1.24 (triangles).

As shown in Fig. 3, the dependence of T_c on the cutoff radius r_n at fixed V_1 rapidly saturates for $n \geq 2$. This can be understood by noting that the long-range ($n \geq 3$) tail of the extended Coulomb potential is strongly suppressed by the metallic screening, while the d-wave pairing wave function is mostly concentrated at 1st-neighbor distance. Hence the effect of the additional ($n > 2$) direct repulsion terms on the pairing is rapidly reduced with increasing r_n. We are thus confident that our conclusions based on finite-range ($n \leq 4$) models are not fundamentally altered in the infinite-range $1/r$ model.

For comparison, we have also explored the effects of an added extended Coulomb repulsion on the d-wave T_c in recently proposed phenomenological spin fluctuation exchange models [15,16]. The d-wave pairing is much more rapidly suppressed with V_1 in such models, primarily due to the lack of screening, i.e., due to the fact that the spin fluctuation mediated pairing potential, as extracted from fits to experimental data, is "rigid" and does not become modified by the extended Coulomb repulsion.

In summary, we find that, at the level of the FLEX approximation to the one-band Hubbard model, spin fluctuation mediated $d_{x^2-y^2}$ pairing is robust against extended $1/r$ electron-electron Coulomb repulsions of realistic strengths. The extended part of the Coulomb interaction does not cause a significant change in the spin fluctuation spectrum nor in the pairing vertex of the Hubbard model for moderate strengths V_1. The robustness of the model against the inclusion of extended Coulomb terms increases with increasing on-site repulsion U. With increasing real-space cutoff radius r_n, the extended Coulomb effects are almost entirely saturated after the inclusion of the 2nd-neighbor repulsion terms. A strong suppression of $d_{x^2-y^2}$ pairing is found only when the extended Coulomb repulsion strength V_1 becomes so large that it induces CDW instabilities in the $\frac{1}{2}$-filled Mott-Hubbard insulator. The ubiquity of AF SDW order in undoped insulating cuprates appears to rule out the latter scenario.

*Email address: esirgen@uga.edu

[1] For a review of the experiments, see D. J. van Harlingen, Rev. Mod. Phys. **67**, 515 (1995), and references therein.

[2] For a review of the theoretical aspects, see D. J. Scalapino, Phys. Rep. **250**, 329 (1995), and references therein.

[3] N. E. Bickers and D. J. Scalapino, Ann. Phys. (N.Y.) **193**, 206 (1989).

[4] M. S. Hybertsen *et al.*, Phys. Rev. B **41**, 11 068 (1990); C.-X. Chen and H.-B. Schüttler, *ibid.* **43**, 3771 (1991); S. B. Bacci *et al.*, *ibid.* **44**, 7504 (1991).

[5] H.-B. Schüttler and A. J. Fedro, Phys. Rev. B **45**, 7588 (1992).

[6] H.-B. Schüttler *et al.*, cond-mat/9805133.

[7] L. G. Aslamazov and A. I. Larkin, Fiz. Tverd. Tela (Leningrad) **10**, 1104 (1968) [Sov. Phys. Solid State **10**, 875 (1968)].

[8] C.-H. Pao and N. E. Bickers, Phys. Rev. Lett. **72**, 1870 (1994); Phys. Rev. B **49**, 1586 (1994); **51**, 16 310 (1995); C.-H. Pao and H.-B. Schüttler, *ibid.* **57**, 5051 (1998).

[9] G. Esirgen and N. E. Bickers, Phys. Rev. B **55**, 2122 (1997); **57**, 5376 (1998).

[10] W. Hanke and L. J. Sham, Phys. Rev. Lett. **33**, 582 (1974); Phys. Rev. B **12**, 4501 (1975).

[11] N. E. Bickers *et al.*, Int. J. Mod. Phys. B **1**, 687 (1987); Phys. Rev. Lett. **62**, 961 (1989); Phys. Rev. B **43**, 8044 (1991).

[12] V. J. Emery *et al.*, Phys. Rev. Lett. **64**, 475 (1990); T. Barnes and M. D. Kovarik, Phys. Rev. B **42**, 6159 (1990); C. Gazza *et al.*, cond-mat/9803314.

[13] D. J. Scalapino, in *Superconductivity,* edited by R. D. Parks (Marcel Dekker, New York, 1969), Vol. 1; P. B. Allen and B. Mitrovic, in *Solid State Physics,* edited by H. Ehrenreich *et al.* (Academic Press, New York, 1982), Vol. 37, pp. 1–91.

[14] R. Preuss *et al.*, Phys. Rev. Lett. **79**, 1122 (1997).

[15] H.-B. Schüttler and M. R. Norman, Phys. Rev. B **54**, 13 295 (1996).

[16] A. Millis *et al.*, Phys. Rev. B **42**, 167 (1990); P. Monthoux and D. Pines, *ibid.* **49**, 4261 (1994); R. J. Radtke *et al.*, *ibid.* **46**, 11 975 (1992); **48**, 15 957 (1993).